Visualization and investigation of Si–C covalent bonding of single carbon nanotube grown on silicon substrate

YuMeng You,[1] Ting Yu,[1] Johnson Kasim,[1] Hang Song,[2] XiaoFeng Fan,[1] ZhenHua Ni,[1] LianZhen Cao,[2] Hong Jiang,[2] DeZhen Shen,[2] JerLai Kuo,[1] and ZeXiang Shen[1,a)]
[1]*Division of Physics and Applied Physics, School of Physical and Mathematical Sciences, Nanyang Technological University, 1 Nanyang Walk, Block 5, Level 3, Singapore 637616, Singapore*
[2]*Key Laboratory of Excited State Processes, Changchun Institute of Optics, Fine Mechanics and Physics, Chinese Academy of Sciences, Changchun 130033, People's Republic of China*

(Received 3 June 2008; accepted 18 August 2008; published online 11 September 2008)

It has been predicted that the electronic properties of carbon nanotubes (CNTs) can be dramatically tuned by forming Si–C bonds with a silicon surface. Thus, the realization of Si–C bonds will broaden future applications of CNTs on nanodevices. In this paper, we use micro-Raman imaging and spectroscopy to investigate the interaction between individual CNTs and silicon substrate. We show that covalent bonds were formed between certain CNTs and the substrate, and visualized such Si-CNT bonds using micro-Raman imaging. Polarized Raman results further reveal that the Si–C bonds are arranged orderly along the long axis of the Si-CNT. We thus show that Raman imaging is a very useful technique to study properties of such Si-CNTs. © *2008 American Institute of Physics*. [DOI: 10.1063/1.2980402]

Carbon nanotubes (CNTs) have attracted a great amount of interest because of their extraordinary electrical, chemical, thermal, and mechanical properties[1–3] that make them promising candidates for nanoelectronics and device applications. One of the unique properties of CNTs is that they can be either metallic or semiconducting, depending on their chirality and diameters.[4] CNTs can also be tuned to be either P-type or N-type by introducing structural defects.[5] Nano-*PN* junctions and nano-field-effect transistors are some of the most fascinating applications[6] that make use of these properties. Recently, many groups have predicted that the electrical properties of single CNTs can be tuned by inducing covalent bonds between the CNTs and a Si substrate.[7–10] By selectively forming covalent bonds between the CNTs and the Si substrate, it is possible to build nanoscaled or even single-molecule electronic devices. Fabrication of CNT devices on Si substrates also has the additional advantage of direct integration into well-developed silicon technology.

However, direct observation of Si–C covalent bonding on single CNTs on Si substrate has not been reported, partly because the lack of suitable characterization techniques. It has been predicted that the Si-CNT interaction results in a large variety of changes in the electronic structures of the CNT. For example, Albrecht and Lyding[7] and Miwa *et al.*[8] studied single-walled CNTs adsorbed on partially and fully hydrogenated Si (001) surfaces.[7,8] They showed that by removing a few H atoms along the adsorption sites, the metallic character of the CNTs will be enhanced. However, removing all the H atoms will render the CNTs semiconducting. To realize Si-CNT devices, the first step is to induce Si-CNT covalent bonds on a large scale. Whatever the technique used to characterize the sample, it must be able to identify the CNTs with Si–C bonds. In this study, we used Raman imaging[11] that can probe down to the submicron scale to investigate isolated single CNTs and their interaction with the Si substrate. The CNTs were grown on silicon substrate at high temperature in order to achieve Si-CNT bonding, and Raman imaging reveals that some single CNTs were covalently attached to the silicon wafer surface.

The CNTs were grown on Si substrate by thermal chemical vapor deposition. The substrate was cleaned using trichloroethylene, acetone, and ethanol in turn by ultrasonic agitation. An ultrathin Fe film, which acted as a catalyst, was deposited in vacuum of 10^{-5} Torr by ion beam sputtering. The substrates were preannealed at 850 °C in hydrogen in a quartz tube furnace for 90 min. CNTs were then grown at 1000 °C for 20 min using methane, hydrogen, and argon at a gas flow rate of 75, 20, and 100 SCCM (SCCM denotes standard cubic centimeter per minute at STP) respectively. The sample was cooled below 300 °C before exposing to air to avoid damage due to rapid cooling.

Raman spectroscopy and imaging were carried out using a WITec CRM200 confocal Raman system with an OLYMPUS microscope objective lens (100×, numerical aperture =0.95). A double-frequency Nd:YAG (yttrium aluminum garnet) laser (532 nm, 100 mW, CNI Laser) was used as the excitation source.

Figure 1(a) shows the scanning electron microscope (SEM) image of the sample. It can be seen that all the CNTs were horizontally grown on the Si substrate in random orientations. The various diameters of CNTs may be due to the different sizes of the Fe catalyst. With the help of markings on Si substrate, Raman imaging was performed on the same region as shown by the SEM image. Careful analysis of the Raman spectra in the Raman images reveal that the Raman spectra of the CNTs shown in Fig. 1(a) can be separated into two groups: those consisting only normal CNT peaks and those with additional peaks which can be assigned to Si–C bonds (to be discussed in detail later). For simplicity, we call these two types of spectra as CNT spectra and Si-CNT spectra, respectively. Figure 1(b) shows the typical Raman spectra of these two groups and that of bulk crystalline SiC for comparison. The CNT spectrum only shows the Raman bands of normal CNTs: the *D* band at 1344 cm^{-1}, the 2*D* band at 2681 cm^{-1}, and the G band.[12] The *G* band can be

a)Author to whom correspondence should be addressed. Electronic mail: zexiang@ntu.edu.sg.

 © 2008 American Institute of Physics

Author complimentary copy. Redistribution subject to AIP license or copyright, see http://apl.aip.org/apl/copyright.jsp

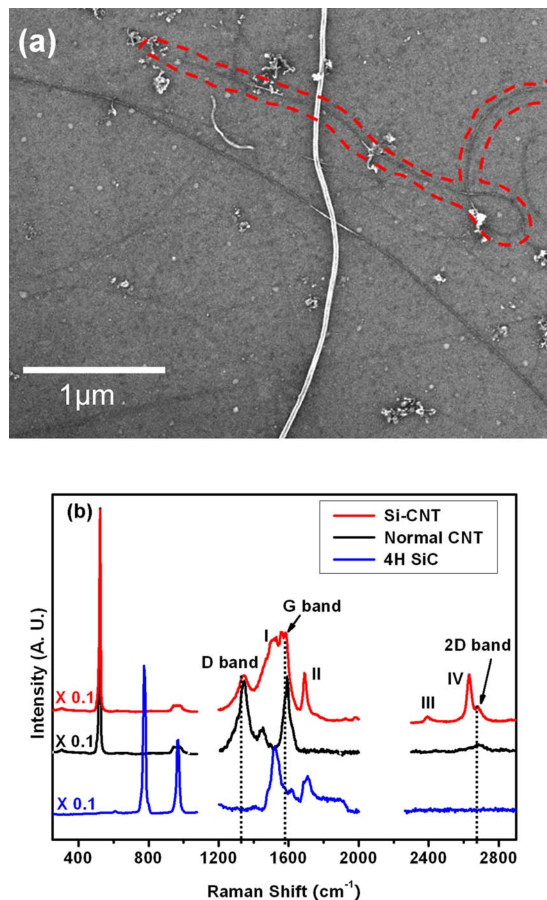

FIG. 1. (Color online) (a) SEM image showing an area of interest. Raman bands belonging to Si–C bonds can be detected on the CNT indicated by the dashed curve in red. (b) Comparison of Raman spectra obtained on normal CNTs (black spectrum), on the special CNT (red spectrum), and on bulk crystalline 4*H* SiC (blue spectrum). The dotted lines represent the CNT peak positions at the *D* band, *G* band, and 2*D* band.

further resolved into the G^- band at 1570 cm^{-1} and G^+ band at 1590 cm^{-1}. For certain CNTs [such as the CNT highlighted by the dashed curve in red in Fig. 1(a)], their Raman spectra show extra bands belonging to Si–C bonds at around 1510 cm^{-1} (band I), 1692 cm^{-1} (band II), 2392 cm^{-1} (band III), and 2620 cm^{-1} (band IV). Several regions were tested in this work and we noted that the extra bands (band I–IV) were observable only for certain CNTs, suggesting that Si–C bonds form only for certain CNTs. We term these CNTs with such bonding as Si-CNTs.

We performed Raman imaging in the backscattering configuration at the same region shown in Fig. 1(a) using a scanning step size of 50 nm and with the incident laser polarized horizontally as indicated by the green arrow in Fig. 2. Raman images constructed using the intensities of different peaks were shown in Figs. 2(a)–2(d). Figure 2(a) was generated by the *G* band (including the G^+ and G^- bands around 1580 cm^{-1}) intensity of CNTs. Brighter regions represent the CNTs, whose locations correspond well with those observed under SEM. We also constructed images using the intensity of the extra band (labeled I) and the resulting image is shown in Fig. 2(b). The shape and position of the bright region matches perfectly the CNT emphasized by the dashed curve in the SEM image [Fig. 1(a)]. Images generated using bands II–IV, shown in Figs. 2(c)–2(e) respectively, exhibit nearly identical patterns as that generated using band I, clearly in-

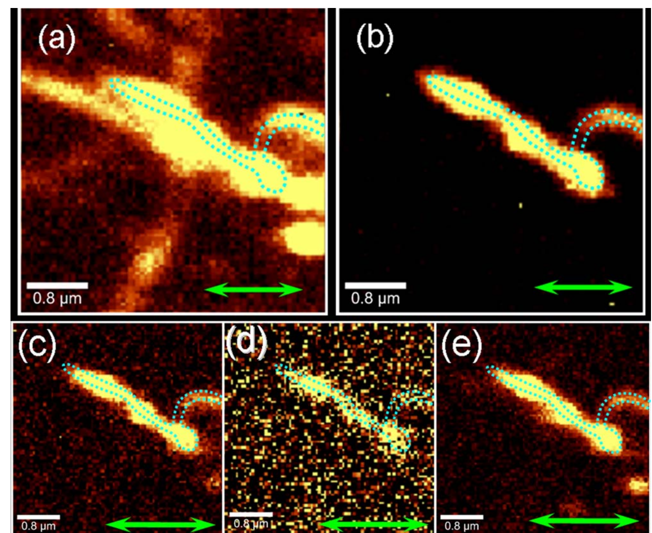

FIG. 2. (Color online) Raman images constructed using peak intensity of (a) *G* band of CNTs, (b) band I of Si–C at 1510 cm^{-1}, (c) band II of Si–C at 1692 cm^{-1}, (d) band III at 2392 cm^{-1}, and (e) band IV at 2620 cm^{-1}. The green arrow indicates the polarization of the incident laser. The blue dotted curves indicate the position and shape of the special CNT.

dicating that the three bands are all correlated with the same CNT emphasized in the SEM image.

Before assigning the peaks, we need to first exclude the possibility that Raman bands I–IV are from CNTs. Band I has a similar shape and position as the fanolike lineshape of the *G* band of metallic CNTs. Oron-Carl *et al.*[13] found that for metallic tubes, the fanolike band has a width around 34–54 cm^{-1}, while for the G^+ band, the width is 20–30 cm^{-1}. For our case, band I has a width of about 130 cm^{-1}, which is much broader than the G^- band in their results. Based on this, we can eliminate the possibility that band I is related to the *G* band of metallic CNTs. Furthermore, as far as we know, the maximum intensity of such fanolike band usually appears around 1540–1550 cm^{-1},[13–16] while band I is found at 1510 cm^{-1}. For band II, we note that the position is similar to that of the band observed in pristine CNTs located around 1740 cm^{-1}. The latter is a combination mode comprising of the first order radial breathing mode (RBM) and the most intense *G* mode (usually the G^+ mode).[17] This peak is normally found together with another band of comparable intensity around 1900 cm^{-1}, which is a combination mode comprising of the second order RBM and the most intense *G* mode. In our experiments, we did not observe such a band near 1900 cm^{-1} and neither did we observe band II on the "normal" CNTs. Hence, we conclude that band II did not originate from the CNTs. In Fig. 1(b) for the spectrum taken at the same position as the Si-CNT, the *D* band is located at 1350 cm^{-1} while both band IV and the 2*D* band of CNTs are located in the region between 2600 and 2800 cm^{-1}. We assigned the bands based on the fact that the frequency of the 2*D* band should be two times the frequency of the *D* band (1350 cm^{-1}). Therefore the 2*D* band should be at 2700 cm^{-1}, as labeled in Fig. 1(b).

To further confirm that these bands in Fig. 1(b) are indeed related to Si-CNT covalent bonds, we compared our Raman spectra with those of bulk crystalline 4*H* SiC which have been well studied.[18] The Raman spectra of bulk crystalline 4*H* SiC are shown, as blue curves in Fig. 1(b). The peak positions and relative intensities of SiC Raman bands

Author complimentary copy. Redistribution subject to AIP license or copyright, see http://apl.aip.org/apl/copyright.jsp

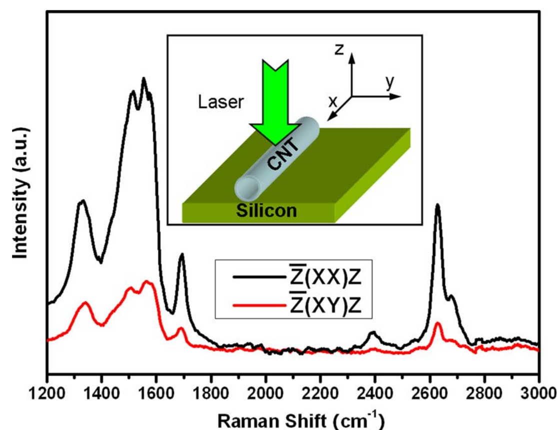

FIG. 3. (Color online) Polarized Raman spectra on the special CNT. Inset is the schematic of the configuration of the experiment.

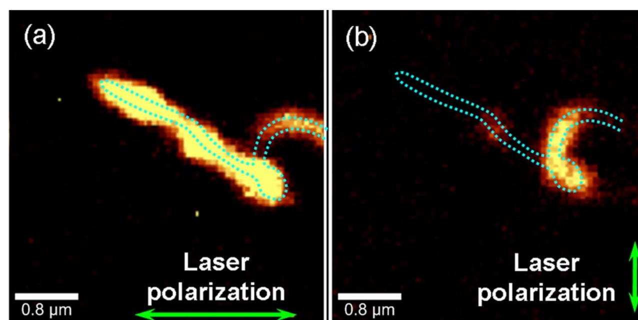

FIG. 4. (Color online) Raman imaging with different incident polarization: (a) horizontal and (b) perpendicular. The blue dotted curves indicate the position and shape of the CNTs with Si–C bonds.

vary for different polytypes, and generally there are two characteristic bands in the region above 1300 cm^{-1}: a broad band between 1510 and 1540 cm^{-1} and a narrower band around 1710 cm^{-1}. Both bands correspond to multibands resulting from overlapping of different overtone phonon vibrations of SiC.[19,20] As shown in Fig. 1(b), the shapes and intensities of band I (1510 cm^{-1}) and band II (1692 cm^{-1}) resemble those of the two characteristic bands of SiC. We noticed that bands III and IV are not detected in bulk SiC at the high frequency region. These spectral differences are understandable considering the following: the Si–C covalent bonds in our case are intrinsically of an interfacial/surface mode, for which the Raman selection rules may be broken down. However, the excellent correspondence in the Raman images constructed by bands III and IV with those constructed by band I and II shows that bands III and IV are also from the Si–C bonds in our sample.

Figure 3 shows the polarized Raman spectra from the CNT with Si–C bonds, with the incident laser polarization along the long axis of the CNT and the Raman signal collected parallel and perpendicular to the polarization of the laser. The results show that the Raman spectra are strongly polarization dependent, which indicate that the Si–C bonds are arranged orderly along the long axis of the Si-CNT.[21] It effectively excludes the possibility that the Si-CNT bands we observed are from surface-adsorbed carbon or other surface contamination, which are normally amorphous with bonds randomly arranged.

Raman imaging with different laser polarizations is also carried out on the area of interest, as shown in Fig. 4. Images are constructed by the peak intensity of band I at 1510 cm^{-1}, one of the second order Raman band of Si-CNT covalent bonding. From the images, it is clear that only the portion of the Si-CNT which has a component parallel to the polarization of the incident laser can be observed. This result can be well explained by the depolarization effect,[22] as the distribution of Si-CNT covalent bonds also follow the anisotropic geometry of the CNTs. The same polarization dependence was also observed for the images constructed from intensities of bands II at 1700 cm^{-1} and IV at 2630 cm^{-1} (results not shown).

In summary, we have grown CNTs on a silicon substrate at high temperature using Fe as the catalyst. Raman spectroscopy and imaging show that Si–C bonds were formed between some CNTs and the Si substrate. Polarized Raman spectroscopy was also carried out, which further verified our conclusion. Systematic investigation of the mechanism of forming such Si-CNT covalent bonds and the vibrational properties of such a system is currently being performed both experimentally and theoretically. We have shown that Raman imaging is a powerful tool for the identification and characterization of individual Si-CNTs bond formation. This is crucial for developing single-CNT nanoscale electronics and logic circuits with tunable electrical transport properties.

[1] S. Iijima, Nature (London) **354**, 56 (1991).
[2] S. J. Tans, M. H. Devoret, H. J. Dai, A. Thess, R. E. Smalley, L. J. Geerligs, and C. Dekker, Nature (London) **386**, 474 (1997).
[3] Y. W. Zhu, F. C. Cheong, T. Yu, X. J. Xu, C. T. Lim, J. T. L. Thong, Z. X. Shen, C. K. Ong, Y. J. Liu, A. T. S. Wee, and C. H. Sow, Carbon **43**, 395 (2005).
[4] R. Saito, M. Fujita, G. Dresselhaus, and M. S. Dresselhaus, Appl. Phys. Lett. **60**, 2204 (1992).
[5] M. Bockrath, J. Hone, A. Zettl, P. L. McEuen, A. G. Rinzler, and R. E. Smalley, Phys. Rev. B **61**, R10606 (2000).
[6] Z. Yao, H. W. C. Postma, L. Balents, and C. Dekker, Nature (London) **402**, 273 (1999).
[7] P. M. Albrecht and J. W. Lyding, Nanotechnology **18**, 125302 (2007).
[8] R. H. Miwa, W. Orellana, and A. Fazzio, Appl. Phys. Lett. **86**, 213111 (2005).
[9] F. D. Mota and C. M. C. de Castilho, Phys. Rev. B **74**, 165408 (2006).
[10] G. W. Peng, A. C. H. Huan, L. Liu, and Y. P. Feng, Phys. Rev. B **74**, 235416 (2006).
[11] A. Mews, F. Koberling, T. Basche, G. Philipp, G. S. Duesberg, S. Roth, and M. Burghard, Adv. Mater. (Weinheim, Ger.) **12**, 1210 (2000).
[12] H. Hiura, T. W. Ebbesen, K. Tanigaki, and H. Takahashi, Chem. Phys. Lett. **202**, 509 (1993).
[13] M. Oron-Carl, F. Hennrich, M. M. Kappes, H. V. Lohneysen, and R. Krupke, Arch. Hist. Exact Sci. **5**, 1761 (2005).
[14] S. D. M. Brown, P. Corio, A. Marucci, M. A. Pimenta, M. S. Dresselhaus, and G. Dresselhaus, Phys. Rev. B **61**, 7734 (2000).
[15] J. Maultzsch, S. Reich, U. Schlecht, and C. Thomsen, Phys. Rev. Lett. **91**, 087402 (2003).
[16] C. Jiang, K. Kempa, J. Zhao, U. Schlecht, U. Kolb, T. Basch, M. Burghard, and A. Mews, Phys. Rev. B **66**, 161404 (2002).
[17] S. D. M. Brown, P. Corio, A. Marucci, M. S. Dresselhaus, M. A. Pimenta, and K. Kneipp, Phys. Rev. B **61**, R5137 (2000).
[18] D. Olego and M. Cardona, Phys. Rev. B **25**, 1151 (1982).
[19] J. C. Burton, L. Sun, F. H. Long, Z. C. Feng, and I. T. Ferguson, Phys. Rev. B **59**, 7282 (1999).
[20] W. Windl, K. Karch, P. Pavone, O. Schutt, D. Strauch, W. H. Weber, K. C. Hass, and L. Rimai, Phys. Rev. B **49**, 8764 (1994).
[21] J. Frechette and C. Carraro, J. Am. Chem. Soc. **128**, 14774 (2006).
[22] G. S. Duesberg, I. Loa, M. Burghard, K. Syassen, and S. Roth, Phys. Rev. Lett. **85**, 5436 (2000).

Author complimentary copy. Redistribution subject to AIP license or copyright, see http://apl.aip.org/apl/copyright.jsp